



Angle-domain least-squares migration through analytical angle-domain Hessian

Wei Zhang and Mauricio D. Sacchi

Signal Analysis and Imaging Group (SAIG), Department of Physics, University of Alberta

Summary

This study presents an angle-domain least-squares migration (LSM) method through the computation of an analytical angle-domain Hessian. We explicitly compute the angle-domain Hessian matrix using the angle-domain Kirchhoff migration and invert it using the inversion technique. The total variation (TV) regularization along the spatial direction and a smoothness constraint along the angle direction are incorporated to suppress migration artifacts. Through numerical experiments with synthetic data, we test the effectiveness of the proposed method and highlight two key benefits. The proposed LSM method can efficiently and effectively recover the high-resolution and high-fidelity angle domain common image-gathers (ADCIGs) in the case of inhomogeneous velocity. It demonstrates the capability to interpolate ADCIGs of sparse recorded data while maintaining reliable amplitude fidelity.

Introduction

Recovering a high-fidelity and high-resolution image of the subsurface reflectors by seismic migration is an indispensable step in seismic exploration. Least-squares migration (LSM), which formulates seismic imaging as a linear inverse problem, has recently become the tool of choice to image complex subsurface targets. LSM can be implemented with different migration engines: Kirchhoff migration (Schuster, 1993), one-way wave-equation migration (Wang and Sacchi, 2007), and reverse time migration (Chen and Sacchi, 2020). This linear inverse problem can be formulated in the data-domain (Schuster, 1993; Wang and Sacchi, 2007) or image-domain (Valenciano et al., 2006; Zhang et al., 2024a, 2025).

Currently, the image-domain LSM methods focus on inverting for the angle-independent reflectivity image or velocity perturbation, with less attention given to the angle-dependent reflectivity image or angle-domain common-image gathers (ADCIGs) (Biondi and Symes, 2004; Wang and Sacchi, 2007; Zhang et al., 2024a,b). This study presents an angle-domain LSM method through the analytical computation of the angle-domain Hessian to reconstruct high-resolution and high-fidelity ADCIGs from the prestack reflection recordings. This inverse problem is formulated in the image domain with the help of an explicit angle-domain Hessian matrix by the wave-equation Kirchhoff migration. One challenge we often face is that angle-domain LSM inversion is a highly ill-conditioned problem. Hence, we used an angle-dependent ℓ_1 norm and a total variation regularization to stabilize the solution to mitigate the angle-dependent wavelet stretching effects and suppress migration artifacts.

Angle-domain LSM

The cost function of angle-domain LSM with the angle-dependent ℓ_1 and TV regularization can be expressed as

$$E_1(\mathbf{r}) = \frac{\lambda_{L2}}{2} \|\mathbf{M}\mathbf{r} - \mathbf{r}_{mig}\|_2^2 + \frac{\lambda_\theta}{2} \|\mathbf{L}_\theta \mathbf{r}\|_2^2 + \sum_{\theta} \frac{\lambda_{L1}(\theta)}{2} \|\mathbf{r}_\theta\|_1 + \frac{\lambda_{TV}}{2} \|\mathbf{r}\|_{TV}, \quad (1)$$

where \mathbf{r}_θ denotes the contribution of ADCIGs at a given reflection angle θ , \mathbf{L}_θ denotes the second-order difference operator along the reflection angle direction of the ADCIGs, and λ_θ denotes the regularization parameter. The proposed regularization scheme includes a second-order difference along the direction of the reflection angle to largely suppress migration artifacts in the migrated ADCIGs. The TV regularization term $\|\mathbf{r}\|_{TV}$ aims to promote spatial smoothness in the inverted image, which helps preserve the structural continuity of the inverted image while reducing migration artifacts. The parameter λ_{TV} adjusts the strength of the TV regularization term. The norm $\sum_{\theta} \frac{\lambda_{L1}(\theta)}{2} \|\mathbf{r}_\theta\|_1$ denotes the angle-dependent ℓ_1 regularization term, promoting vertical sparsity in the inverted image, which helps in improving the vertical resolution of the inverted ADCIGs by mitigating wavelet stretching. The regularization parameter $\lambda_{L1}(\theta)$ adjusts the strength of the sparsity constraint at the different reflection angles.

The angle-dependent ℓ_1 regularization extends traditional sparse regularization by incorporating the angle-dependent regularization parameter. As a comparative method, the objective function with the standard ℓ_1 sparse regularization term can be expressed as

$$E_2(\mathbf{r}) = \frac{\lambda_{L2}}{2} \|\mathbf{M}\mathbf{r} - \mathbf{r}_{mig}\|_2^2 + \frac{\lambda_\theta}{2} \|\mathbf{L}_\theta \mathbf{r}\|_2^2 + \frac{\lambda_{L1}}{2} \|\mathbf{r}\|_1 + \frac{\lambda_{TV}}{2} \|\mathbf{r}\|_{TV}. \quad (2)$$

where the deconvolution imaging condition can be used to compute the migrated ADCIGs

$$r_{mig}(\mathbf{x}, \theta) = \frac{2}{v(\mathbf{x})} \int d\omega i\omega \int d\mathbf{x}_r \int d\mathbf{x}_s g(\theta, \theta_x) \times \frac{G(\mathbf{x}, \mathbf{x}_s, \omega) G(\mathbf{x}, \mathbf{x}_r, \omega) d_{obs}^*(\mathbf{x}_r, \mathbf{x}_s, \omega) \cos(\theta_x)}{G^*(\mathbf{x}, \mathbf{x}_s, \omega) G(\mathbf{x}, \mathbf{x}_s, \omega) + \varepsilon}, \quad (3)$$

where $g(\theta, \theta_x)$ denotes a weighting function. The Hessian matrix can be derived from the cascade operator of forward modelling and migration:

$$M(\mathbf{x}, \theta, \mathbf{y}) = \frac{4}{v(\mathbf{x})v(\mathbf{y})} \int d\omega \omega^2 F^*(\omega) \int d\mathbf{x}_r \int d\mathbf{x}_s \times \frac{G(\mathbf{x}, \mathbf{x}_r, \omega) G(\mathbf{x}, \mathbf{x}_s, \omega) \cos(\theta_x) g(\theta, \theta_x)}{G(\mathbf{x}, \mathbf{x}_s, \omega) G^*(\mathbf{x}, \mathbf{x}_s, \omega) + \varepsilon} \times G^*(\mathbf{y}, \mathbf{x}_r, \omega) G^*(\mathbf{y}, \mathbf{x}_s, \omega) \cos(\theta_y). \quad (4)$$

In this study, we compute the full-wave Green function using the excitation amplitude and traveltimes full wavefields (Nguyen and McMechan, 2013). When we set $\mathbf{y} = \mathbf{y}_0$ and reshape the Hessian into the image-space, we obtain the so-called angle-domain imaging resolution function (IRF) $M(\mathbf{x}, \theta, \mathbf{y}_0)$.

Results: A Graben model

In this experiment, we use the Graben velocity model. In this model, the absolute values of angle-dependent reflection coefficients are the same, differing only in polarity. Figure 1 displays the re-

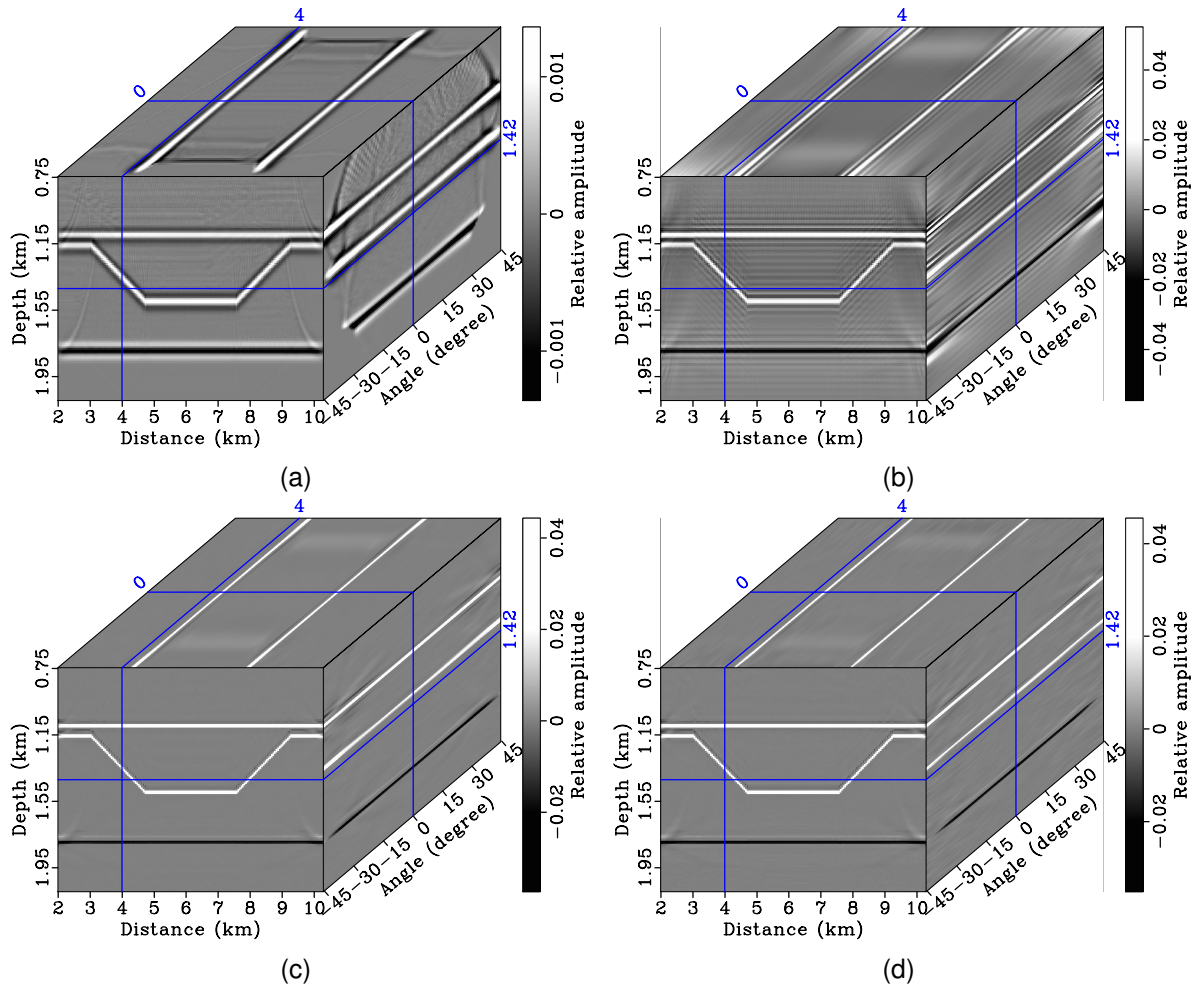


Figure 1: The ADCIGs for the Graben model from different methods. (a) Angle-domain KM, (b) angle-domain LSM with the L2 regularization, (c) angle-domain LSM with the L2 and standard L1 regularizations, (d) angle-domain LSM with the L2 and angle-dependent L1 regularizations.

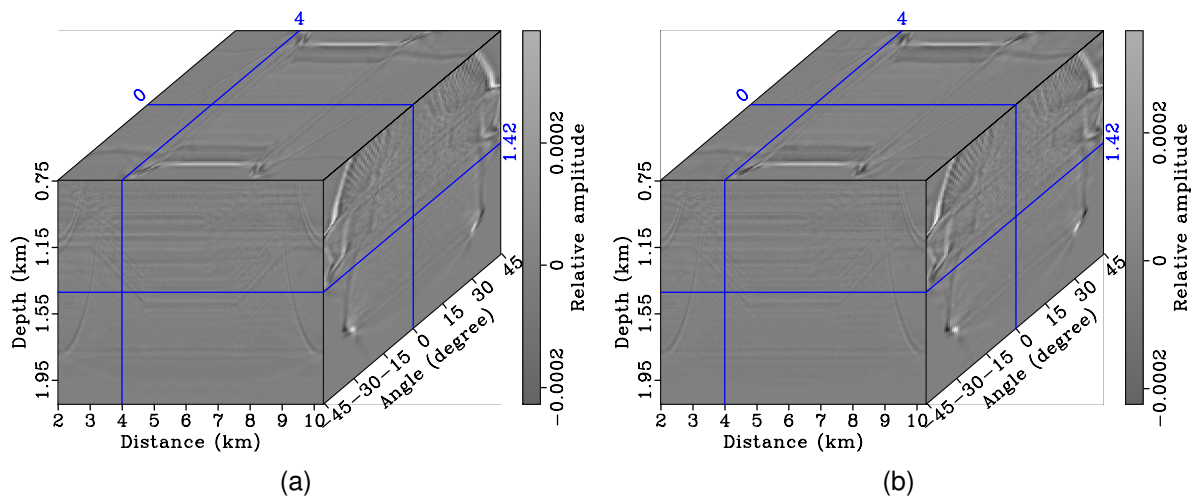


Figure 2: (a) The residual of the image-matching term in Figure 1c and (b) the residual of the image-matching term in Figure 1d.

covered ADCIGs for a Graben model using different methods. We can provide the following insights from the recovered ADCIGs: (1) The angle-domain LSM with the ℓ_2 regularization in Figure 1b, angle-domain LSM with the ℓ_2 and standard ℓ_1 regularizations in Figure 1c, angle-domain LSM with the ℓ_2 and angle-dependent ℓ_1 regularizations in Figure 1d can improve the quality of ADCIGs from angle-domain Kirchhoff migration in Figure 1a. The imaging resolution has been improved to varying degrees for the different methods. The migration artifacts of ADCIGs caused by the limited recording aperture have been completely suppressed in all the angle-domain LSM methods. The image-matching residual contains some far-field migration artifacts visible in Figures 2a and 2b. The migrated ADCIGs from angle-domain Kirchhoff migration exhibit a significant angle-dependent wavelet stretching effect, especially at large angles. The inversion techniques in angle-domain LSM can mitigate this effect to some extent. (2) The angle-domain LSM with the ℓ_2 regularization suffers from the well-known sidelobes artifacts around reflectors in Figure 1b. The oscillation of reflected events will reduce the vertical resolution of the migrated image. By imposing the standard ℓ_1 regularization, these sidelobes artifacts around reflectors can be largely removed in Figure 1c. (3) The inversion technique with the standard ℓ_1 regularization can mitigate this angle-dependent wavelet stretching effect. It can be observed that this stretching effect still exists in the inverted image in Figure 1c. Especially at large angles, the residual sidelobe artifacts around reflectors are still present. The high-resolution reflectivity image can be recovered at different reflection angles by imposing the angle-dependent ℓ_1 regularization proposed in this paper. The wavelet-dependent effects can be almost completely removed in Figure 1d.

Conclusions

This study presents an angle-domain LSM method through the analytical computation of an angle-domain Hessian. We explicitly compute the angle-domain Hessian matrix using the angle-domain Kirchhoff migration and invert it using iterative inversion. We obtained three insights through a synthetic example based on a Graben model. The first is that LSM can compensate for the illumination effects that distort imaging ADCIGs and recover closer to the true amplitude image. The second one is that sparse regularization must be applied to LSM to stabilize the inversion solution and suppress migration noise. The third point is that the angle-dependent ℓ_1 norm needs to be added to remove the angle-dependent stretching effect in ADCIGs. Similarly, experiments have been conducted for multi-parameter LSM with encouraging results.

Acknowledgements

We want to thank the Signal Analysis and Imaging Group sponsors at the University of Alberta for supporting the stimulating research environment that allowed the preparation of this work.

References

- Biondi, B., and W. Symes, 2004, Angle-domain common-image gathers for migration velocity analysis by wavefield-continuation imaging: *Geophysics*, **69**, R1283–R1298.
- Chen, K., and M. D. Sacchi, 2020, Time-domain elastic gauss–newton full-waveform inversion: a matrix-free approach: *Geophysical Journal International*, **223**, 1007–1039.
- Nguyen, B. D., and G. McMechan, 2013, Excitation amplitude imaging condition for prestack reverse-time migration: *Geophysics*, **78**, S37–S46.
- Schuster, G. T., 1993, Least-squares cross-well migration: SEG Technical Program Expanded Abstracts, 110–113.
- Valenciano, A. A., B. Biondi, and A. Guitton, 2006, Target-oriented wave-equation inversion: *Geophysics*, **71**, A35–A38.
- Wang, J., and M. D. Sacchi, 2007, High-resolution wave equation avp imaging with sparseness constraints: *Geophysics*, **72**, S11–S18.
- Zhang, W., X. Guo, M. Ravasi, J. Gao, and W. Sun, 2024a, Angle-dependent image-domain least-squares migration through analytical point spread functions: *Geophysics*, **89**, S339–S360.
- Zhang, W., X. Guo, Y. Shi, X. Ke, L. Song, J. Gao, and H. Chen, 2025, Suppressing migration artifacts using angle-domain least-squares migration: *IEEE Transactions on Geoscience and Remote Sensing*, **63**, 1–13.
- Zhang, W., M. Ravasi, J. Gao, and Y. Shi, 2024b, Deep-unrolling architecture for image-domain least-squares migration: *Geophysics*, **89**, S215–S234.